Proceedings World Geothermal Congress 2020+1
Reykjavik, Iceland, April - October 2021

Benefits from Subsurface Urban Heat Islands to Shallow Geothermal Applications – an Example from the City of Cologne, Germany

Hannes Hemmerle[1], Ingo Dressel[1], Philipp Blum[2], Kathrin Menberg[2], Susanne A. Benz[3], Peter Bayer[1]

[1]Ingolstadt University of Applied Sciences, Institute of new Energy Systems (InES), Ingolstadt, Germany

[2]Karlsruhe Institute of Technology (KIT), Institute of Applied Geosciences (AGW), Karlsruhe, Germany

[3]University of California San Diego, School of Global Policy and Strategy (GPS), La Jolla, CA 92093, USA

mail@bayerpeter.com

Keywords: groundwater temperature, remote sensing, geothermal heat potential, urban hydrology

ABSTRACT

In urbanized areas subsurface temperatures are often elevated in comparison to surrounding rural areas. These anthropogenic distortions of the thermal field are usually referred to as subsurface urban heat islands (SUHI) that typically show a positive offset of several degrees Celsius. Shallow geothermal heating systems benefit especially from this non-uniform but often large scale temperature rise. Therefore, SUHIs have an elevated geothermal potential. Accessing this thermal energy yields an eco-friendly and cost-efficient option to meet the enormous local heating demand in cities. Recycling the long-term anthropogenic heat emission by geothermal use also reduces the thermal disturbance in the subsurface and brings underground conditions a step closer to the natural state. Besides the ecological compatibility, shallow geothermal applications have to be competitively viable in economic terms. In the present study, the additional theoretical geothermal heat potential (TGP) of the SUHI beneath the city of Cologne, Germany, is quantified by estimating groundwater temperatures from satellite data and building footprints. The described estimation of urban subsurface temperature is robust with a root-mean squared error (RMSE) of 0.86 K. Anthropogenic heat emissions into the subsurface beneath Cologne accumulated to an additionally stored heat that could theoretically meet the cities heating demand for almost 3 years without taking any sources of recharge into account. Satellite based estimation techniques can be a crucial tool in quantifying this replenishing resource, which could play an important role in future heat production.

1 INTRODUCTION

Most geothermal applications are small scale heat-pump based devices that are operated in residential and built-up areas. These are most often used for heating and thus benefit from the enormous geothermal energy potential that is found in the shallow subsurface of cities (Bayer et al. 2019). In fact, many cities, especially in colder climates, also reveal themselves to be regions of elevated ground and groundwater temperatures. The temperatures measured in such “subsurface urban heat islands” (SUHIs) are several degrees warmer than in the rural surrounding, caused by permanent heat release from basements of buildings, subsurface infrastructure, district heating and sewage pipes, as well as by accelerated heat flux from streets and sealed surfaces (Ferguson and Woodbury 2007, Shi et al. 2012, Menberg et al. 2013b, Benz et al. 2015). For city-wide use of the shallow subsurface for the purpose of heating, elevated temperatures mean an increased geothermal potential (Zhu et al. 2010, Rivera et al. 2015, Epting 2017, Sliwa et al. 2019). Also, efficiencies of borehole heat exchangers increase with the ground temperature when used for heat extraction. Finally, geothermal heat extraction can also serve as means for mitigation of further urban subsurface heating, which may cause thermal stress to soil, groundwater and groundwater ecosystems (Brielmann et al. 2011, Possemiers et al. 2014).

Urban regions commonly have a high density of boreholes and wells, which can be used to map the thermal subsurface regime and thus estimate the elevated geothermal potential. In most cases, however, no integrated monitoring programs of urban ground (water) temperature exist. Even if measurement campaigns are conducted, the number of logged wells is rarely sufficient for high-resolution mapping of subsurface temperatures. Therefore, the aid of easily available remote sensing data has been suggested to approximate the thermal conditions beneath the land surface by the information sensed at the surface (Zhan et al. 2014, Benz et al. 2015, Benz et al. 2017a, b, Hemmerle et al. 2019). This is motivated by the strong coupling between land surface and soil temperature, as well as by the role of the land use for the observed ground (water) temperature. Green spaces often manifest as relatively cool regions, whereas asphalted and built-up areas are associated with higher subsurface temperatures, as a consequence of enhanced ground heat input (Zhu et al. 2015, Rivera et al. 2016, Cermak et al. 2017). For rural areas, Benz et al. (2017a) were able to predict groundwater temperatures (GWT) with a root mean squared error (RMSE) of 1.4 K using a global dataset of GWT measured in wells worldwide. In urban areas, GWT of shallow aquifers can be estimated well when accounting for building density (BD). This was demonstrated for the city of Paris (Hemmerle et al. 2019) and four German cities including Cologne (Benz et al. 2015).

The present work builds upon these previous GWT estimation methods and presents an application to the city of Cologne, Germany, which has already been subject to earlier studies (Zhu et al. 2010, Menberg et al. 2013a, Benz et al. 2015, Zhu et al. 2015, Shao et al. 2017). The goal is to derive a new and more reliable estimation of the urban GWT and the associated geothermal potential by assimilation of remotely sensed land surface information. With this, the purpose is also to provide a more reliable support for other concepts that are applied for spatial planning of geothermal energy use of the shallow urban ground (Zhang et al. 2015, Epting et al. 2017, Tissen et al. 2019).

2. METHODS AND DATA

2.1 Field measurements

Temperature profiles were measured in groundwater at 72 wells in October 2009 using temperature logging equipment (SEBA KLL-T) with an accuracy of 0.1 K. The field methodology is described by Zhu et al. (2010). In order to mitigate effects from seasonal ground temperature variation, only groundwater temperatures (GWT) at a depth of 20 m are considered. Therefore, wells reported by Zhu et al. (2010) but shallower than 20 m are ignored in this study. The location of the remaining 57 wells is illustrated in Figure 1.

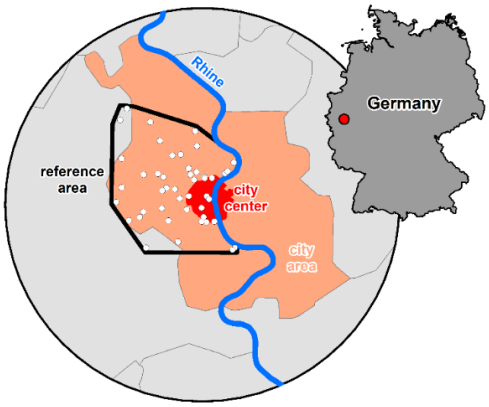

Figure 1: Map of Cologne with sampling wells (white dots) and location of the city (red dot) in Germany (dark gray outline in the top right). City center (red) and city area (light red) are simplified representations of the municipal areas. The reference area (black line) delineates the approximate study area of Zhu et al. (2010). As illustrated, the map is cropped to a 15 km radial buffer around the city center.

2.2 Estimating groundwater temperature in mixed environments

Recently, satellite data were used to estimate groundwater temperature by calculating a functional relationship (i.e. an offset) between measured GWT and corresponding land surface temperature (LST). For a global dataset of 2548 GWTs located in natural environments, Benz et al. (2017a) were able to roughly predict shallow subsurface temperature by correcting LST for latent heat flow from evapotranspiration (ET) and the thermal insulation on days with snow covered surface (SD – snow days). The resolution of the Global Land Data Assimilation System (GLDAS) ET data (Rodell et al. 2004) used by Benz et al. (2017a) is only 0.25 arc degrees (approx. 28 km). Such coarse resolution, however, is not suitable for estimating spatially variable groundwater temperatures on a city-scale. For example, in the case of Cologne, one raster cell would cover the entire city area. On account of this, we use here the Terraclimate data (Abatzoglou et al. 2018) which has a resolution of 2.5 arc minutes (approx. 4.6 km). Another option would be the new MODIS version 6 ET product (Running et al. 2017) with a ground resolution of 500m × 500m. However, data coverage in urban areas is almost zero in this dataset, which makes it useless for the purpose of this study.

Following the procedure described by Benz et al. (2017a), we performed a multiple linear regression (without fitting the y-intercept) on the same global dataset, which results in equation 1 for rural estimated groundwater temperature ($eGWT_r$) in °C:

$$eGWT_r = LST + 7.17\ [K] \cdot SD + 3.24 \cdot 10^4\ [K\ s\ mm^{-1}\ ] \cdot ET \quad (1)$$

where LST is the annual mean from MODIS Version 6 Aqua and Terra LST daily product in °C (MODIS 2019), SD is the percentage of days with snow cover from the MODIS Version 5 Aqua and Terra satellite (Hall et al. 2006), and ET is the actual evapotranspiration from Terraclimate data in mm s^{-1}. For the global data set, the associated root mean squared error is RMSE = 1.39 K. Regression using the Terraclimate data predicts a slightly lower impact of ET on GWT than the previous version relying on GLADS data with $\Delta T_{ET} = 3.24 \cdot 10^4\ [K\ s\ mm^{-1}\ ] \cdot ET_{Terraclimate}$ compared to $\Delta T_{ET} = 3.5 \cdot 10^4\ [K\ s\ mm^{-1}\ ] \cdot ET_{GLDAS}$ while at the same time a slightly higher impact of snow is predicted ($\Delta T_{SD} = 7.17\ [K] \cdot SD$ compared to ($\Delta T_{SD} = 6.6\ [K] \cdot SD$).

In urban environments subsurface temperature is additionally altered by anthropogenic thermal emissions. A variety of different sources contribute to subsurface warming, such as building basements, subsurface infrastructure, and sewage systems, among many others. To compensate for these thermal impacts, the estimation approach is corrected for regions of intense anthropogenic land and subsurface use. These areas usually contain a high amount of built-up area. Therefore, the building density (BD) is used as a proxy for the anthropogenic heat emission into the subsurface. An ordinary least square regression for BD is performed on the difference between measured GWT in Cologne and $eGWT_r$ at the corresponding location. While a y-intercept should not exist under ideal conditions, it was included here to reflect the expected errors caused by e.g. clear sky bias in the observed satellite data and the observation of snow, primarily on roofs. This results in equation 2, which gives a local estimation technique that is also capable of estimating GWT in mixed (urban and rural) environments:

$$eGWT = eGWT_r + 6.28\ [K] \cdot BD - 1.16. \quad (2)$$

Building densities are calculated from Open Street Map polygons on a 1 km × 1 km grid. Building footprints were accessed via the OSMnx python package (Boeing 2017). For each grid cell, the polygon area coverage is calculated and divided by the raster area (1 km^2).

2.3 Theoretical geothermal potential (TGP)

The geothermal potential of cities recently received increasing attention. For this study, we will focus on the theoretical geothermal potential (TGP), which is usually defined as the total energy stored in an adiabatically closed reservoir (Bayer et al. 2019). In the context of SUHIs, the additional TGP due to urbanization thus can be defined as the additional energy (or heat) in place depending on the temperature change induced by urbanization (ΔT)

$$TGP = (n \cdot c_w + (1 - n) \cdot c_s) \cdot A \cdot d \cdot \Delta T \quad (3)$$

where n, c_s, c_w, A, d, are porosity, volumetric heat capacity of solid, volumetric heat capacity of water, area, and aquifer thickness, respectively. In agreement with Zhu et al. (2010), we used n = 0.2, d = 20 m, c_s = 2.1 MJ m^{-3} K^{-1}, and c_w = 4.15 MJ m^{-3} K^{-1}.

Equation 2 is applied to a 1km × 1km gridded point cloud within a 15 km buffer around the center of Cologne (Figure 4) to spatialize eGWT. The buffer area contains 699 grid-points, which is negligibly smaller than the expected area of a circle with a radius of 15 km (706.9 km^2). The observed offset is due to clipping and coordinate systems conversions. Before applying equation 3 to calculate TGP, the temperature change induced by urbanization is calculated as $\Delta T = eGWT - GWT_0$ for each point, where eGWT is the estimated groundwater temperature and GWT_0 is the undisturbed rural groundwater temperature.

A separation between rural and urban land use is required to define GWT_0. Grid cells were split into urban and rural pixels by using the Global Human Settlement Layers (GHSL) Settlement Grid (Pesaresi and Freire 2016). These data provide the degree of urbanization with values of 0 to 3, which represent uninhabited, rural, low-density urban, and high density urban land-use, respectively. In this scope, uninhabited, rural, and low-density urban class (0, 1, 2) are defined as rural for determining GWT_0. Hereby, 176 pixels are classified as rural and 523 pixels as urban.

All raster data, except those describing the building density, are downloaded and processed with Google Earth Engine (Gorelick et al. 2017). LST, SD, and ET (equation 1) are computed as mean values for the time period from 2005 to 2014. GHSL data is representative for the year 2014. For a more detailed description on raster computing and processing via Google Earth Engine, please refer to Benz et al. (2017a) and Hemmerle et al. (2019).

3 RESULTS AND DISCUSSION

3.1 Estimated groundwater temperatures (eGWT)

Statistical figures for the 57 wells at a depth of 20 m are listed in Table 1. The measured GWT in Cologne ranges between 10.8 and 16.3 °C, with the highest temperature located directly in the city center. In the following, the measured groundwater temperature (GWT) is compared to land surface temperature (LST), an estimation of rural groundwater temperatures ($eGWT_r$ – equation 1), and a combined estimation of groundwater temperatures in urban and rural areas (eGWT – equation 2). Figure 2 shows the correlation between GWT and LST, $eGWT_r$, and eGWT separately. The corresponding misfit is characterized by the root mean squared error (RMSE), which represents the overall error of estimation. Additionally, the mean error (ME), which describes the bias of the data, and the spearman correlation coefficient are concerned. Land surface temperature and measured GWT yield a RMSE of 1.37 K and a ME of -0.75 K, which indicates that groundwater temperature is noticeably underestimated by LST. Compared to the plain use of LST, RMSE and ME for the rural estimate, $eGWT_r$ are decreased to 1.19 K and 0.09 K, accordingly. For the calibrated estimate (eGWT) the RMSE is below 1 K at 0.86 K. The Spearman correlation coefficient (r) is also highest for eGWT with 0.67 K. The ME is zero as a result of the linear regression fitting. Besides misfit measures, eGWT is much more capable of producing relatively high temperatures in the city center with the maximum eGWT being 15.4 °C, which still is slightly below the measured GWT.

Table 1: Mean value, standard deviation (σ), and descriptive statistics of 57 wells for measured groundwater temperature (GWT), land surface temperature (LST), rural estimated groundwater temperature ($eGWT_r$), calibrated estimated groundwater temperature (eGWT), and induced temperature differences (ΔT) of the estimation approach. ΔT is split into contribution from correction by building densities (ΔT_{BD}), evapotranspiration (ΔT_{ET}) and snow cover (ΔT_{SD}).

	mean	σ	min	25%	50%	75%	max
GWT /°C	12.6	1.3	10.8	11.6	12.3	13.1	16.3
LST /°C	11.8	0.6	10.5	11.5	11.7	12.2	12.8
$eGWT_r$ /°C	12.6	0.5	11.5	12.2	12.6	13.0	13.5
eGWT /°C	12.6	1.1	10.4	11.7	12.6	13.3	15.4
ΔT_{BD} /K	1.12	0.81	-0.00	0.51	0.88	1.59	3.15
ΔT_{ET} /K	0.62	0.01	0.59	0.61	0.61	0.63	0.64
ΔT_{SD} /K	0.17	0.10	0.07	0.10	0.12	0.22	0.45

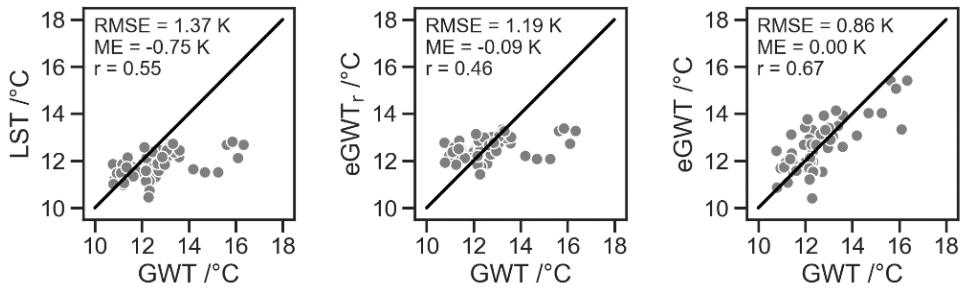

Figure 2: Measured groundwater temperature (GWT) vs. land surface temperature (LST), rural estimated groundwater temperature ($eGWT_r$), and calibrated estimated groundwater temperature (eGWT). Root-mean squared error (RMSE), mean error (ME) and spearman correlation coefficient (r) for each subplot are displayed in the upper left corner.

The induced spatial temperature differences by the different datasets are depicted in Figure 3. The difference between LST and eGWT is a composite of four factors: (**1**) the y-axis intercept ε = -1.16 K of the BD ordinary least square regression (equation 2); (**2-4**) the differences induced by SD, ET, and BD (ΔT_{SD}, ΔT_{ET}, ΔT_{BD}). ΔT_{SD} yields the smallest correction with a mean value of 0.17 K. ΔT_{ET} is second smallest and more or less constant for the data with a standard deviation of σ = 0.01 K and a mean value of 0.62 K. ΔT_{BD} has the highest impact on eGWT with a correction range between 0 and 3.15 K.

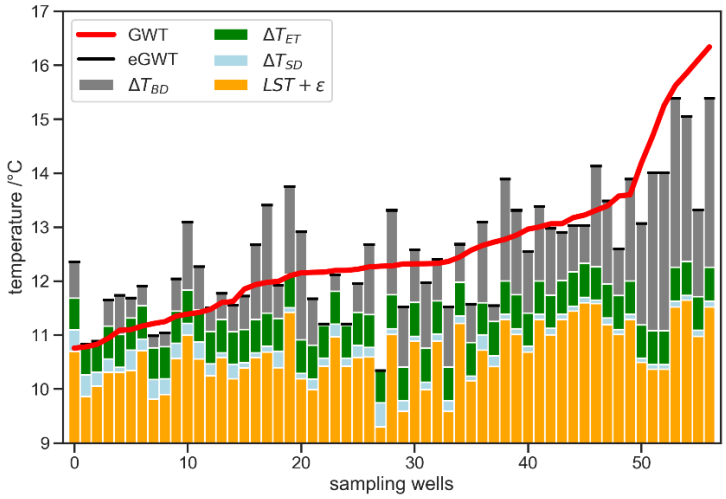

Figure 3: Measured groundwater temperature (GWT) and estimated groundwater temperature (eGWT) for 57 wells in Cologne at 20 m below surface. Bars give the contribution from temperature correction by the different raster sets (ΔT_{SD}, ΔT_{ET}, ΔT_{BD}) for each well location, added to the land surface temperature (LST) corrected with the local offset (ε= -1.16 K).

Besides the 15 km arbitrary buffer area, the municipal region of the city of Cologne (city area), the city center of Cologne, and a reference area, which was used for a previous estimation of the geothermal potential (Zhu et al. 2010), are investigated (Figure 1). There are minor discrepancies in the delineation of the reference area (below 5% spatial variation), while the total area is equal over 140 km². In addition, the areas classified as urban and rural by the degree of urbanization (Pesaresi and Freire 2016) are distinguished (Figure 4).

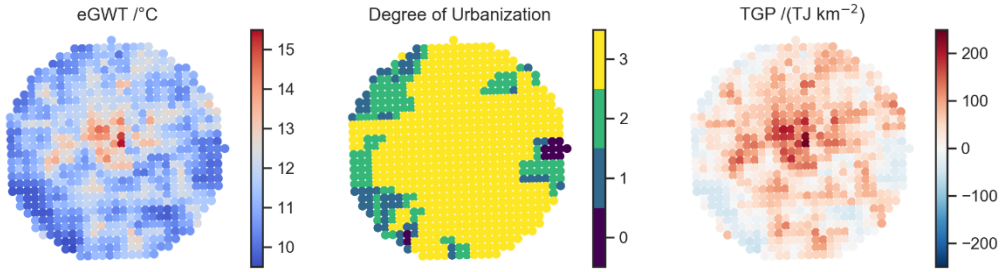

Figure 4: Estimated groundwater temperature (eGWT), degree of urbanization and theoretical geothermal potential (TGP). Data is gridded on a 1 km × 1 km raster with a radius of 15 km around Cologne city center (same extent as Figure 1).

Subsurface urban heat island intensities (SUHII) are a common way to describe SUHIs in a generalized and comparative way. The two most common procedures are calculating a minimum-maximum SUHII ($SUHII_{max\text{-}min} = eGWT_{max} - GWT_0$) where the minimum represents the rural unaltered groundwater temperature, and by the difference between the 10% and 90% quantile ($SUHII_{90\text{-}10}$). The second option was presented by Menberg et al. (2013a) and is less prone to very local heating effects, but thus also neglects extreme values. GWT_0 is set as the median value of all rural eGWT (10.6 °C). Further eGWT statistics for the six different areas are given in Table 2. For the city area, the $SUHII_{max\text{-}min}$ is 4.8 K and the $SUHII_{90\text{-}10}$ is 2.5 K indicating a substantial SUHI beneath the city of Cologne. Over the 15 km buffer region eGWT ranges from 9.5 °C to 15.4 °C.

Table 2: Estimated groundwater temperatures (eGWT), subsurface urban heat island intensity (SUHII), and theoretical geothermal potential (TGP) for the city center, city area, reference area, and 15 km buffer area (Figure 1), as well as for an alternative classification into rural and urban land use.

	city center	reference area	city area	15 km buffer	urban area	rural area
Area /km²	16	140	405	699	523	176
$eGWT_{min}$ /°C	11.0	10.4	9.7	9.5	9.5	9.6
$eGWT_{mean}$ /°C	13.0	12.2	11.6	11.4	11.7	10.7
$eGWT_{median}$ /°C	12.8	12	11.6	11.4	11.7	10.6
$eGWT_{max}$ /°C	15.4	15.4	15.4	15.4	15.4	12.9
$SUHII_{max\text{-}min}$ /°C	4.8	4.8	4.8	4.8	4.8	2.3
$SUHII_{90\text{-}10}$ /°C	2.7	2.5	2.5	2.4	2.2	1.7
TGP /PJ	2.0	11.6	21.3	29.5	28.8	0.7
TGP_{mean} /(TJ km^{-2})	122.7	82.8	52.6	42.2	55	4.1

3.2 Theoretical geothermal potential (TGP)

The theoretical geothermal potential (TGP) for the six different areas is given in Table 2. For the city area, the total TGP is 21.3 PJ with a mean value of 52.6 TJ km^{-2}. With the annual heating demand for Cologne being 19 TJ km^{-2} a^{-1} (Zhu et al. 2010), the anthropogenic subsurface heat loss could potentially supply the heating demand of Cologne for 2.8 years without recharge. For the city center the TGP per area is much higher with 122.7 TJ km^{-2} compared to 52.6 TJ km^{-2} for the city area. This is due to the elevated subsurface temperatures in the city center.

To validate the remote sensing approach, we compare the presented findings to previous results by Zhu et al. (2010), who derived the TGP by interpolating measured subsurface temperatures on a 500 m × 500 m raster within the reference area. In the following, the TGP calculated by Zhu et al. (2010) is referred to as TGP_i where 'i' indicates interpolation of groundwater temperatures, and the TGP calculated in this study is referred to as TGP_e, where 'e' indicates the estimation of groundwater temperature from satellite data.

The given range of the previous TGP_i for the reference area is 9.8 to 11 PJ, while the TGP_e is slightly higher with 11.6 PJ. The average TGP_i per area is 70 to 79 kJ km^{-2}, while the average TGP_e is also higher at 82.8 kJ km^{-2}. As TGP mainly depends on $\Delta T = eGWT - GWT_0$, absolute values have a strong influence by the rural background temperature GWT_0. Setting GWT_0 from the observed rural median temperature of 10.6 °C to the minimum observed value of 10.8 °C given by Zhu et al. (2010) would decrease TGP_e to 10.2 PJ in total and 72.6 kJ km^{-2} per area within the reference area. Hereby, the TGP_e would have an offset of 2% from the average TGP_i of the previous estimate, while still being within the given range for TGP_i. Besides the fact that the remote sensing based method in this case provides similar results, the RMSE for estimating groundwater temperatures is still close to 1 K. However, taking into account errors for interpolation methods on city-scale, this error is acceptable.

The presented results are very promising as the remotely sensed method is able to produce nearly the same TGP values when compared to previous results. However, when applying the presented estimation approach, some requirements have to be met. The local rural GWT reference (GWT_0) needs to be carefully set with a consistent methodology, as it has a high impact on the total TGP. Also, we assume that GWT does not vary vertically within the aquifer and that the temperature at 20 m below surface represents the temperature in the aquifer. Furthermore, seasonal and annual aquifer temperature variation is assumed to be negligible with respect to the RMSE = 0.86 K for estimating the groundwater temperature.

Furthermore, limitations of this approach have to be considered. (**1**) No small scale temperature variations can be displayed due to the raster size of 1 km × 1 km. Local temperature variability is typically very high in urban environments and can differ by several K within one grid cell. (**2**) This estimation has by definition a strong dependence on local calibration to BD. Therefore, it is not easily applicable to other cities without further local calibration. (**3**) A lot of assumptions had to be made (e.g. porosity, aquifer thickness) for making a city-wide prediction of the geothermal potential. With other methods relying on the same assumptions, these can also be seen as systematic errors and will not alter results significantly, as the theoretical geothermal potential solely depends on the offset of urban groundwater temperature to the undisturbed rural groundwater temperature. (**4**) Measured groundwater temperatures are not homogenously distributed over the 15 km buffer area. Therefore, the local calibration could have a bias towards areas with high sampling density.

4 CONCLUSION AND OUTLOOK

Groundwater temperature (GWT) for the city of Cologne is estimated with an RMSE of 0.86 K. The proposed method is capable of describing the respective SUHI in spatial extent and intensity. Based on the estimated value, eGWT, the theoretical geothermal potential (TGP) is calculated on the city scale. Without taking into account any thermal recharge, the estimated TGP beneath the city

is 2.8 times the annual heating demand of Cologne. Despite all uncertainties in remote sensing, alternatives to this approach also suffer from different problems. Previously used interpolation methods (e.g. kriging or nearest neighbor) rely on simple interpolation of field data. Therefore, they are not capable of estimating uninvestigated areas and require a rather homogeneous sample distribution. Numerical flow and heat transport models on the other hand are prone to overfitting and do require a lot of computational power as well as careful parametrization. However, they are capable of resolving GWT at a higher resolution and are generally preferred to solve small scale local problems.

The biggest surplus of remote sensing, is that it can easily be transferred to other cities and is the most viable option, when it comes to making a quick and cost efficient estimation of GWT, or for quantifying the TGP. In a next step, similar approaches may be applied to a wider dataset of European cities to make a comparative analysis of the TGP in general.

ACKNOWLEDGEMENTS

We thank Jakob Michael for language editing. This work is funded by the German Research Foundation (grant number BA2850/3-1).

REFERENCES

Abatzoglou, J.T., Dobrowski, S.Z., Parks, S.A., and Hegewisch, K.C.: TerraClimate, a high-resolution global dataset of monthly climate and climatic water balance from 1958–2015, *Scientific data,* **5**, (2018), 170191.

Bayer, P., Attard, G., Blum, P., and Menberg, K.: The geothermal potential of cities, *Renewable and Sustainable Energy Reviews,* **106**, (2019), 17-30.

Benz, S.A., Bayer, P., and Blum, P.: Global patterns of shallow groundwater temperatures, *Environmental Research Letters,* **12**, (2017a), 034005.

Benz, S.A., Bayer, P., and Blum, P.: Identifying anthropogenic anomalies in air, surface and groundwater temperatures in Germany, *Science of The Total Environment,* **584**, (2017b), 145-153.

Benz, S.A., Bayer, P., Goettsche, F.M., Olesen, F.S., and Blum, P.: Linking surface urban heat islands with groundwater temperatures, *Environmental science & technology,* **50**, (2015), 70-78.

Boeing, G.: OSMnx: New methods for acquiring, constructing, analyzing, and visualizing complex street networks, *Computers, Environment and Urban Systems,* **65**, (2017), 126-139.

Brielmann, H., Lueders, T., Schreglmann, K., Ferraro, F., Avramov, M., Hammerl, V., Blum, P., Bayer, P., and Griebler, C.: Oberflächennahe Geothermie und ihre potenziellen Auswirkungen auf Grundwasserökosysteme, *Grundwasser,* **16**, (2011), 77.

Cermak, V., Bodri, L., Kresl, M., Dedecek, P., and Safanda, J.: Eleven years of ground–air temperature tracking over different land cover types, *International Journal of Climatology,* **37**, (2017), 1084-1099.

Epting, J.: Thermal management of urban subsurface resources-Delineation of boundary conditions, *Procedia engineering,* **209**, (2017), 83-91.

Epting, J., García-Gil, A., Huggenberger, P., Vázquez-Suñe, E., and Mueller, M.H.: Development of concepts for the management of thermal resources in urban areas–assessment of transferability from the Basel (Switzerland) and Zaragoza (Spain) case studies, *Journal of hydrology,* **548**, (2017), 697-715.

Ferguson, G., and Woodbury, A.D.: Urban heat island in the subsurface, *Geophysical research letters,* **34**, (2007),

Gorelick, N., Hancher, M., Dixon, M., Ilyushchenko, S., Thau, D., and Moore, R.: Google Earth Engine: Planetary-scale geospatial analysis for everyone, *Remote Sensing of Environment,* **202**, (2017), 18-27.

Hall, D., Salomonson, V., and Riggs, G.: MODIS/Terra snow cover daily L3 global 500m grid, *Boulder, Colorado USA: National Snow and Ice Data Center (Version 5.[Tile h09v04])*, (2006),

Hemmerle, H., Hale, S., Dressel, I., Benz, S.A., Attard, G., Blum, P., and Bayer, P.: Estimation of Groundwater Temperatures in Paris, France, *Geofluids,* **2019**, (2019),

Menberg, K., Bayer, P., Zosseder, K., Rumohr, S., and Blum, P.: Subsurface urban heat islands in German cities, *Science of The Total Environment,* **442**, (2013a), 123-133.

Menberg, K., Blum, P., Schaffitel, A., and Bayer, P.: Long-term evolution of anthropogenic heat fluxes into a subsurface urban heat island, *Environmental science & technology,* **47**, (2013b), 9747-9755.

MODIS: MODIS-LST-V6-Aqua and MODIS-LST-V6-Terra, (2019),

Pesaresi, M., and Freire, S.: GHS Settlement grid following the REGIO model 2014 in application to GHSL Landsat and CIESIN GPW v4-multitemporal (1975-1990-2000-2015), *JRC Data Catalogue*, (2016),

Possemiers, M., Huysmans, M., and Batelaan, O.: Influence of Aquifer Thermal Energy Storage on groundwater quality: A review illustrated by seven case studies from Belgium, *Journal of Hydrology: Regional Studies,* **2**, (2014), 20-34.

Rivera, J.A., Blum, P., and Bayer, P.: Ground energy balance for borehole heat exchangers: vertical fluxes, groundwater and storage, *Renewable energy,* **83**, (2015), 1341-1351.

Rivera, J.A., Blum, P., and Bayer, P.: Influence of spatially variable ground heat flux on closed-loop geothermal systems: Line source model with nonhomogeneous Cauchy-type top boundary conditions, *Applied energy,* **180**, (2016), 572-585.

Rodell, M., Houser, P., Jambor, U., Gottschalck, J., Mitchell, K., Meng, C.-J., Arsenault, K., Cosgrove, B., Radakovich, J., and Bosilovich, M.: The global land data assimilation system, *Bulletin of the American Meteorological Society,* **85**, (2004), 381-394.

Running, S., Mu, Q., and Zhao, M.: MOD16A2 MODIS/Terra Net Evapotranspiration 8-Day L4 Global 500m SIN Grid V006, *NASA EOSDIS Land Processes DAAC https://doi. org/10.5067/MODIS/MOD16A2,* **6**, (2017),

Shao, H., Hein, P., Bucher, A., and Kolditz, O. 2017. Technically exploitable geothermal energy by using Borehole Heat Exchangers: A revisit of the Cologne case. Page 8379 *in* EGU General Assembly Conference Abstracts.

Shi, B., Tang, C.-S., Gao, L., Liu, C., and Wang, B.-J.: Observation and analysis of the urban heat island effect on soil in Nanjing, China, *Environmental earth sciences,* **67**, (2012), 215-229.

Sliwa, T., Sojczyńska, A., Rosen, M.A., and Kowalski, T.: Evaluation of temperature profiling quality in determining energy efficiencies of borehole heat exchangers, *Geothermics,* **78**, (2019), 129-137.

Tissen, C., Menberg, K., Bayer, P., and Blum, P.: Meeting the demand: geothermal heat supply rates for an urban quarter in Germany, *Geothermal Energy,* **7**, (2019), 9.

Zhan, W., Ju, W., Hai, S., Ferguson, G., Quan, J., Tang, C., Guo, Z., and Kong, F.: Satellite-derived subsurface urban heat island, *Environmental science & technology,* **48**, (2014), 12134-12140.

Zhang, Y., Soga, K., Choudhary, R., and Bains, S. 2015. GSHP application for heating and cooling at 'City Scale'for the city of westminster.*in* Proceedings World Geothermal Congress.

Zhu, K., Bayer, P., Grathwohl, P., and Blum, P.: Groundwater temperature evolution in the subsurface urban heat island of Cologne, Germany, *Hydrological processes,* **29**, (2015), 965-978.

Zhu, K., Blum, P., Ferguson, G., Balke, K.-D., and Bayer, P.: The geothermal potential of urban heat islands, *Environmental Research Letters,* **5**, (2010), 044002.